Korean J. Chem. Eng., **31**(4), 664-675 (2014)
DOI: 10.1007/s11814-013-0243-0

pISSN: 0256-1115
eISSN: 1975-7220

Polyelectrolyte complexes of chitosan self-assembled with fucoidan: An optimum condition to prepare their nanoparticles and their characteristics

Eun Ju Lee* and Kwang-Hee Lim*,,†**

*Department of Chemical Engineering, College of Engineering, Daegu University, Kyungsan, Gyeongbuk 712-714, Korea
**Laboratory of Pharmaceutical Bio-nanomaterials, Daegu University, Kyungsan, Gyeongbuk 712-714, Korea
(*Received 4 October 2013 • accepted 17 November 2013*)

Abstract−The preparation conditions for both a high yield without aggregation and a small mean-size of chitosan-fucoidan nanoparticles were sought by a screening method, i.e., discarding the ones satisfying neither of both to prepare them by polyelectrolyte complexation with chitosan and fucoidan. The effect of the pH level of chitosan solution and the chitosan-fucoidan mass ratio was investigated on the following aspects: the turbidity and aggregation pattern of suspension, the yield of dried mass, electrostatic interaction, fucoidan loading efficiency, the particle size distribution and the morphology of the polyelectrolyte complex prepared by polyelectrolyte complexation between chitosan and fucoidan. The mean size of prepared nanoparticle ranges between 365-900 nm. The nanoparticles tended to grow as the pH of chitosan was increased up to 3.69, after which they became smaller. This pattern of growth is prominent as the mass ratio of chitosan and fucoidan decrease. The conditions of pH 5 and 1 : 1 chitosan-fucoidan mass ratio were suggested as ad hoc optimum conditions by the screening method to prepare chitosan-fucoidan nanoparticles for high yield, small size and good suspension stability. They were almost consistent with the optimum conditions for the maximum value of chitosan-fucoidan nanoparticles prepared per unit input mass, which were analyzed by response surface methodology (RSM).

Keywords: Nanoparticle, Optimum Condition, Polyelectrolyte Complexation, Chitosan, Fucoidan

INTRODUCTION

The use of polyelectrolyte complexation from oppositely charged macromolecules as controlled drug release formulations has attracted much attention because this process is simple, feasible, and usually performed under mild conditions. Also, since preparation of the complex is through physical crosslinking by electrostatic interactions instead of chemical crosslinking, the possibility of toxicity associated with crosslinking reagents involved in chemical crosslinking processes can be eliminated [1]. Polysaccharides, which are typical polyelectrolytes, have been frequently studied for drug-delivery applications. Among these, chitosan has received increasing attention for a wide range of drug-delivery applications. It is derived from deacetylation of chitin, becoming a linear polyamine with a high ratio of glucosamine to acetyl-glucosamine units (Fig. 1(a)). The solubility of chitosan is dependent on protonation of the amino groups in the molecules; therefore, it is often solubilized in aqueous acids [2]. Protonation of chitosan results in its carrying positive charges and, therefore, to interact with negatively charged polymers and macromolecules. Consequently, chitosan complexation with polyanionic polymer has been widely studied as hydro-gels [3], films [4], beads [5], microparticles [6] and nanoparticles [7].

So far the widely used method to produce chitosan nanoparticles relies on polyelectrolyte complexation: it requires, in addition to chitosan, only such a polyanionic polymer as tripolyphosphate (TPP) [8-16], alginate [7,17], dextran sulfate [2], cellulose-hydrolyzed carboxymethyl cellulose [18], heparin [19,20], DNA [21], glycyrrhetic acid [22], and carboxymethyl konjac glucomannan and poly-gamma glutamic acid [1,23]. Fucoidan is a negatively charged polysaccharide naturally occurring in many species of brown algae and many marine invertebrates; however, the only commercially available form of fucoidan is obtained from the brown algae "*Focus vesiculosus*." Its structure is mainly based on L-fucose with mainly $\alpha(1\rightarrow3)$ glycosidic bonds and sulfate groups at position four [24] (Fig. 1(b)). There have been various *in-vivo* and *in-vitro* studies on

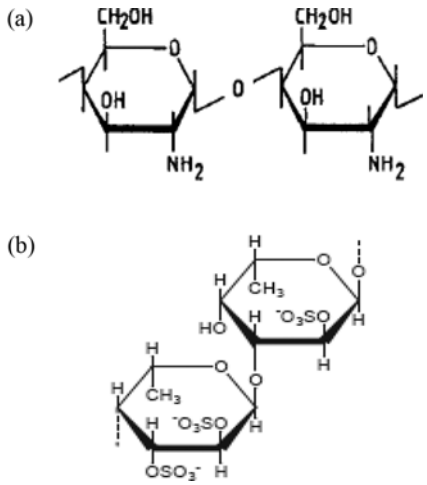

Fig. 1. Chemical structure of basic unit of (a) chitosan and (b) fucoidan.

†To whom correspondence should be addressed.
E-mail: khlim@daegu.ac.kr

the anticarcinogenic effects of fucoidan, which has been known to induce the apoptosis [25-29] or to inhibit the angiogenic activity [30] of some cancer cells. By virtue of its dynamic biological properties fucoidan has been widely reported for its pharmacological activities [31-36].

The submicron size of nanoparticles offers a number of distinct advantages over microparticles, including relatively higher intracellular uptake compared with microparticles. In terms of intestinal uptake, apart from their particle size, their nanoparticle nature and charge properties seem to influence the uptake by intestinal epithelia [37]. By chitosan, in particular, the epithelial cells are facilitated to open their tight junctions for enhancing the absorption of drugs through the oral routes [38]. Yue et al. [39] reported that the surface charge affects cellular uptake and intracellular trafficking of chitosan-based nanoparticles in the way that positively-charged nanoparticles promote the internalization rate due to the positively-charged nanoparticles preferring to contact with negatively-charged cell surface with their electrostatic interaction. Therefore, a smaller-positively charged chitosan nanoparticle is believed optimized to promote the intestinal uptake greater.

The characteristics of chitosan-fucoidan polyelectrolyte complex nanoparticles were originally reported by Lee et al. [40], the authors of this article, using polyelectrolyte complexation between chitosan and fucoidan at various pH conditions of chitosan/fucoidan mixed solution and at various mass ratios of chitosan and fucoidan. A composite hydrogel sheet composed of alginate, chitin/chitosan and fucoidan was prepared as a wound dressing by Murakami et al. [41], which possesses many advantages for the repair of healing-impaired wounds. Huang and Liu [42] prepared chitosan/fucoidan nanoparticles and chitosan/fucoidan/tripolyphosphate nanoparticles to control the release of stromal cell-derived factor-1 for the purpose of regulating the mobilization of stem cells. The curcumin-release using chitosan/fucoidan nanoparticles for oral delivery system has been recently investigated by Huang and Lam [43] at the pH environments of 1.2 (empty stomach), 2.5 (stomach after meal), 6.0 (duodenum), 7.0 (jejunum) and 7.4 (epithelial cells). Mitsumata et al. [44] reported that the degree of swelling increased with elapsed time and reached equilibrium around four days after chitosan, k-carrageenan/NaCMC complex hydrogels were immersed in pure water (pH 7). However, according to Fredheim and Christensen [45], the apparent irreversibility in the reaction between chitosan and lignosulfonate observed when increasing pH after complex formation is attributed to hysteresis, which is commonly observed for precipitation/dissolution of other polyelectrolytes. Thus, it is believed that a crosslinking-charge density of chitosan nanoparticles remains the same in a reasonably short time scale under any pH-environment, unless they are disintegrated, once chitosan nanoparticles are formed by polyelectrolyte complexation. In addition, pH environment-sensitive-equilibrated full swelling or collapsing of chitosan/fucoidan nanoparticles for oral delivery system may not happen quickly within such a relatively short time scale as a transmit time in stomach (10-30 min), duodenum (less than 60 s) and jejunum (3±1.5 hr). Therefore, it becomes important to administer the optimized chitosan/fucoidan nanoparticles to promote the intestinal uptake greater for oral delivery system so that they may be swollen to disintegrate after the process of intestinal uptake. From an economic aspect, the high yield of chitosan-fucoidan nanoparticles is also regarded as an important factor. However, the required condition for a high yield does not always meet the criteria of their preparation condition for the smallest chitosan-fucoidan nanoparticles in a stable suspension. Accordingly, we suggest for the first time the preparation condition satisfying both a high yield without aggregation and a small mean size of positively charged chitosan-fucoidan nanoparticles to promote their intestinal uptake and intracellular trafficking greater for oral delivery system, using the analysis on the following aspects: the turbidity and aggregation pattern of suspension (suspension stability), the yield of dried mass, the particle size distribution, the morphology of their polyelectrolyte complex, and so forth. Subsequently, the optimum conditions are obtained statistically for the maximum value of chitosan-fucoidan nanoparticles prepared per unit input-mass by response surface methodology (RSM). Then, the optimum conditions are compared with the suggested preparation condition. The formation of chitosan-fucoidan nanoparticles is interpreted by correlating characteristics and their charge density. For its validation, a fucoidan loading efficiency is experimentally measured in chitosan-fucoidan nanoparticles prepared under various pH and chitosan-fucoidan mass ratios in their solution.

MATERIALS AND METHODS

1. Preparation of Chitosan-fucoidan Complex Nanoparticles

By dissolving 100 mg of chitosan (deacetylation degree of 75-85%, viscosity (0.5% in 5% acetic acid) of 5-20 cps, case # 0321-6250 Showa chemicals Japan) in 0.2%w/v acetic acid (Merck, Germany), 0.1%w/v chitosan solution was prepared to make the final volume of 100 ml. Five milliliters of 0.1%w/v chitosan solution (in 0.2%w/v acetic acid) was taken in a beaker. To study the effect of the pH level of the chitosan solution, the pH of 5 ml of 0.1%w/v chitosan solution (in 0.2%w/v acetic acid) was adjusted to 2, 3, 5, or 6 with 1 N NaOH or HCl (DC chemical Korea), as per case. Thus, the chitosan solutions were prepared for the pH of 2, 3, 5 and 6 as well as the unadjusted pH of 3.69. In addition 0.1%w/v fucoidan solution was prepared by dissolving 100 mg of fucoidan from *Fucus vesiculosus* (Sigma-Aldrich, case# F5631-1G) in deionized water to make the final volume of 100 ml. Then the dispersion of the chitosan-fucoidan complex was prepared by mixing the positively-charged chitosan and the negatively-charged fucoidan by dropping method. Accordingly, 0.25 ml, 0.5 ml, 1 ml, 2 ml, 3 ml, 4 ml and 5 ml of 0.1%w/v fucoidan solution were added dropwise into the chitosan solution under continuous stirring, to achieve the chitosan-fucoidan ratios of 1 : 0.05, 1 : 0.1, 1 : 0.2, 1 : 0.4, 1 : 0.6, 1 : 0.8 and 1 : 1, respectively. After 30 min of stirring the turbidity of the dispersion was measured by UV-Vis spectrophotometer (UV-1601 PC Shimadzu) and it was centrifuged at 13,000 g for 15 min. The pellets, if any, were re-dispersed in 3 ml water and transferred to empty glass tubes and frozen before freeze drying. After lyophilization with a freeze-dryer (Ilshin Lab Co. Ltd., FD 8512), the yield of the dried mass was calculated gravimetrically. The standard deviation of the yield-errors that occurred from triple-repeated experiments was also calculated as error bars. The morphology of chitosan-fucoidan complex nanoparticles was examined by scanning electron microscopy (Hitachi, S-4300).

2. Measurement of pH

The dispersion of the chitosan-fucoidan complex was prepared at

various pH ranges of chitosan solution. The pH value of the chitosan solution before and after the addition of fucoidan solution was measured at room temperature with a digital pH meter (Istek-720P, Istek Inc.) and its glass electrode. The pH meter was calibrated with three buffer solutions (pH 4, 7 and 10) supplied by Istek Inc.

3. Measurement of Absorbance of Suspension

To estimate the turbidity of the dispersion, the absorbance of the final dispersion was measured, before centrifugation at a 550 nm wavelength using a double beam UV-Vis spectrophotometer (UV-1601 PC, Shimadzu). Deionized-water was run as a blank to zero the absorbance, and the absorbance of the sample was measured at the same wavelength.

4. Calculation of Dried Mass-yield

The empty glass tubes were dried and weighed along with the identification labels pasted on them. This weight was noted as the weight of empty bottles before freeze drying. The redispersed pellets in the centrifugation tubes were transferred to the weighed empty glass tubes and frozen for freeze drying. After freeze drying the tubes were weighed again, and the difference in the weight was taken as the weight of the dried mass. The yield of the dried mass was calculated gravimetrically as follows:

$$\text{Yield} = \frac{\text{weight of dried mass (g)}}{\text{weight of [chitosan + fucoidan] used (g)}} \times 100 \quad (1)$$

5. Estimation of Fucoidan-loading Efficiency

According to the aforementioned recipe of chitosan-fucoidan complex nanoparticles, chitosan-fucoidan complex particles were formed in the chitosan-fucoidan solution of pH 2 and 6. After 30 min of stirring, it was centrifuged at 13,000 ×g for 15 mins. Then the supernatant was collected and treated by 0.2 μm membrane filter (Millipore). The absorbance of the treated supernatant was measured at the wavelength of 420 nm by UV-Vis spectrophotometer (UV-160 PC Shimadzu) to estimate the concentration of remaining fucoidan after chitosan-fucoidan complexation in the solution. The standard curves were calibrated with the absorbance measurement of 0.0125%-0.1%w/v fucoidan solution at the wavelength of 420 nm. Fucoidan-loading efficiency was calculated according to the equation as below.

$$\text{Fucoidan-loading efficiency} = \frac{\text{Fuco}^0 - \text{y}}{\text{Fuco}^0} \quad (2)$$

where

1) Fuco^0 and y denote the fucoidan concentration of mixed chitosan-fucoidan solution before chitosan-fucoidan complex is formed, and its remaining fucoidan concentration after the complex is formed.

2) Fuco^0 is calculated in consideration of the fucoidan concentration before mixing (i.e., 0.1%w/v) and the mixing effect resulted from various chitosan-fucoidan mass ratios.

6. Analysis of Mean Particle Size

The size distribution of suspended hydrogel particles of the chitosan-fucoidan complex, prepared according to the aforementioned recipe, was analyzed by a submicron particle size analyzer (N5/LS-13320, Beckman Coulter).

7. FTIR Spectrum Analysis

FTIR spectrum was recorded on an FTIR Spectrometer (Genesis II, Mattson instrument) to determine the interaction between chitosan and fucoidan. The chitosan-fucoidan complex particles were separated from the suspension by centrifugation. The precipitate was obtained by discarding the supernatant and was frozen before freeze drying. The pellets of freeze-dried mass were prepared according to KBr-pellet techniques and the corresponding FT-IR spectrum was obtained. For each spectrum an interferogram was collected from the 4,000 to 600 cm^{-1} region at room temperature. The spectrum of pure chitosan and fucoidan was also obtained to analyze the interaction involved in the formation of their complex.

8. Optimum Condition for the Maximum Value of Chitosan/Fucoidan Nanoparticles per Unit Input Mass

The first consideration for optimum condition is a notable yield and apparent stability of particle suspension. Therefore, the preparation condition causing either negligible yield or apparent particle aggregation in the suspension was pre-screened and rejected. Then, the second consideration was to define the observations to be fitted to the second order polynomial model. The second order polynomial regression model was used to consider the main effect, quadratic effect and interactive effect of independent variables for regression analysis as follows:

$$\eta = \gamma_o + \gamma_1 x_1 + \gamma_2 x_2 + \gamma_{11} x_1^2 + \gamma_{12} x_1 x_2 + \gamma_{22} x_2^2 \quad (3)$$

where η, x_i, γ_o, γ_i, γ_{ii} and $\gamma_{ij(i\neq j)}$ are a response (i.e., dependent variable), an independent variable, an intercept and regression parameters for main effect, quadratic effect and interactive effect of independent variables, respectively.

The combined observations obtained by Eq. (4) are designated as the values of chitosan-fucoidan nanoparticles prepared per unit input-mass according to the following formula:

$$\alpha = Y\zeta \quad (4)$$

where α, ζ and Y are the value of chitosan-fucoidan nanoparticles prepared per unit input-mass, the value per unit mass of prepared chitosan-fucoidan nanoparticles and yield of chitosan-fucoidan nanoparticles, respectively.

Considering the facilitation of the intracellular uptake of chitosan-fucoidan nanoparticles due to their small size, the value per their unit mass (i.e., ζ) would be greater as their mean size gets smaller. Assuming the value per unit mass of prepared chitosan-fucoidan nanoparticles (i.e., ζ) is inversely proportional to their mean size to the power of n (e.g., 1, 3/2, 2 and 3), the combined observations of the values of chitosan-fucoidan nanoparticles prepared per unit input-mass may be obtained by Eq. (5):

$$\alpha = \beta \frac{Y}{\delta^n} \quad (5)$$

where α, β, Y, δ and n are the value of chitosan-fucoidan nanoparticles prepared per unit input mass, a coefficient, yield of chitosan-fucoidan nanoparticles, the mean size of chitosan-fucoidan nanoparticles and a power index, respectively.

The surface of responses of Eq. (3) was analyzed by RSM using RSREG procedure of SAS ver. 8.2. For the analysis of RSM, the independent variables are designated as pH (i.e., x_1) of chitosan solution and mass ratio (i.e., x_2) of chitosan and fucoidan, while the dependent variable (i.e., response) is η, which corresponds to the combined observations (i.e., α/β x1000) that are 1000 times the value of Y/δ^n. With the 2^2-fractional factorial experimental design, nine data (i.e., 4 factorial points, a center point and four axial points) of experiments performed at various conditions were considered ac-

Table 1. Experimental matrices for central composite design: x_1= pH and x_2=MR (chitosan-fucoidan mass ratio=1: MR)

Experiment number	pH		MR (mass ratio)	
	Coded	Uncoded	Coded	Uncoded
1	−1	3	−1	0.4
2	−1	3	1	0.8
3	1	5	−1	0.4
4	1	5	1	0.8
5	−2	2	0	0.6
6	2	6	0	0.6
7	0	4	−2	0.2
8	0	4	0	0.6
9	0	4	2	1.0

cording to a central composite design (CCD), as shown in Table 1, for the optimization of the surface of responses.

RESULTS AND DISCUSSION

1. Turbidity, Yield and Apparent Turbidity/Aggregation Pattern

The formation and properties of polymer complexes depend on the charge ratio of anionic- to cationic-polymers, the degree of neutralization, the ionic strength, and the valence of simple ions in the electrolyte solution. When fucoidan was dropped into chitosan solution, molecular electrostatic attractions occurred between the anionic sulfate groups of fucoidan and the cationic amino groups of chitosan. These attractions could make the inter-molecular chains of chitosan and fucoidan curl up, which leads to the formation of an insoluble chitosan-fucoidan complex. The charge density of chitosan molecules is dependent on the pH of the solution [9]. The unadjusted pH of 0.1%w/v chitosan solution (in 0.2%w/v acetic acid) and 0.1%w/v fucoidan solution was measured to be 3.69 and 7.08, respectively. In addition, the pH of the final suspension was measured to be almost identical to the corresponding pH of the chitosan solution when the ratio of chitosan-fucoidan was 1 : 0.05. However, it increased slightly by the value between 0.1 and 0.2 as the ratio of chitosan-fucoidan changed from 1 : 0.1 to 1 : 1. The effect of various pH values (i.e., 2, 3, 3.69 (unadjusted), 5 and 6) of chitosan solutions was analyzed with the different chitosan-fucoidan mass ratios (i.e., 1 : 0.05, 1 : 0.1, 1 : 0.2, 1 : 0.4, 1 : 0.6, 1 : 0.8 and 1 : 1) on the characteristics of the formation, and the yield of the polyelectrolyte complex composed of chitosan and fucoidan. In particular, at pH 6 of the chitosan solution, some visible aggregates were observed at the ratio of 1 : 0.6. Nevertheless, the pellets could be redispersed into a turbid suspension containing visible agglomerates. Contrary to the previous lower pH cases, the chitosan-fucoidan ratio of 1 : 0.8 and 1 : 1 apparently led to turbid suspension with visible agglomerates in the system and the pellets obtained after centrifugation could not be redispersed at all. It may be attributed to the system approaching an iso-electric point (IEP), which will be discussed further later in this article. It was observed that the turbidity and the yield of the chitosan-fucoidan complex formation are dependent on the pH of the chitosan solution as well as the chitosan-fucoidan mass ratio, as shown in Figs. 2 and 3. As the pH of the chitosan solution increased, the effect of

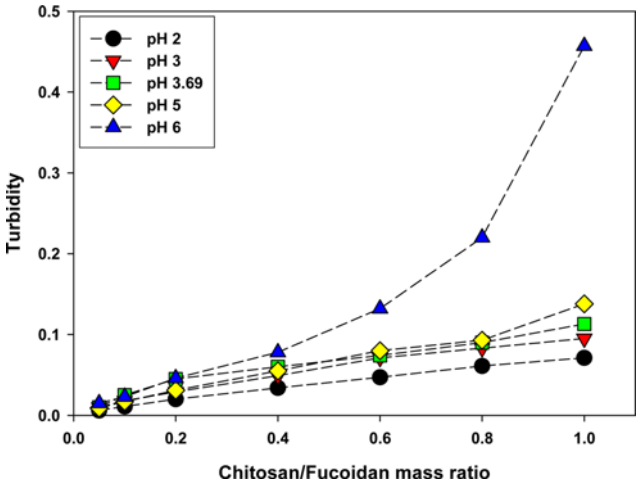

Fig. 2. The effect of chitosan-fucoidan mass ratio on the turbidity of chitosan-fucoidan complex particle formation at various pH.

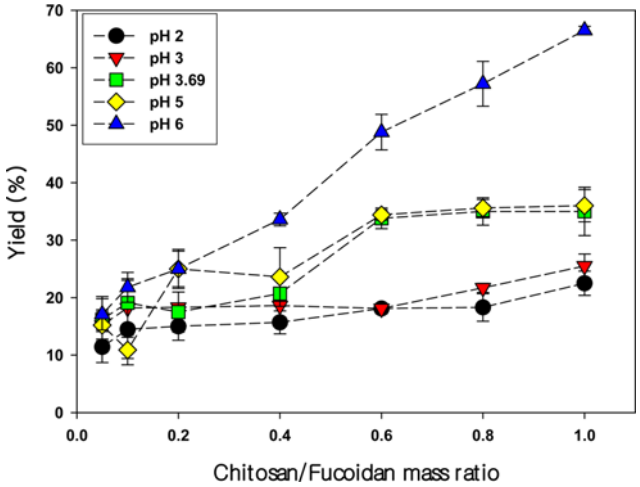

Fig. 3. The effect of chitosan-fucoidan mass ratio on the yield of chitosan-fucoidan complex particle formation at various pH (Error bars in the figure stand for standard deviations of the errors occurred from triple measurements).

the chitosan-fucoidan mass ratio became greater on the turbidity and the yield of the chitosan-fucoidan complex. However, according to Table 2 the apparent turbidity/aggregation pattern was found not to be affected by the pH of the chitosan solution except for the pH of 6.

2. Correlation between Charge Density of Chitosan-fucoidan Nanoparticles and their Formation

The solubility of chitosan is dependent on protonation of the amino groups in the molecules, so it is often solubilized in aqueous acids [2]. Protonation of chitosan results in its carrying positive charges. The positively charged chitosan may interact with the negatively charged fucoidan. The dissociation constants of chitosan and fucoidan have been known as ca. 6.5 [46] and 1-2.5 [47], respectively. Accordingly, their charge densities are affected by the pH values of chitosan solution. At the pH 6 of the chitosan solution the protonation of the amino groups is less effective and the positive charge density of each chitosan molecule becomes less than those at the lower pH of the chitosan solution. However, the concentration of

Table 2. Apparent turbidity/aggregation pattern of chitosan-fucoidan complex dispersion at various pH and mass ratios

pH	Chitosan-fucoidan mass ratio						
	1 : 0.05	1 : 0.1	1 : 0.2	1 : 0.4	1 : 0.6	1 : 0.8	1 : 1
2	×/×	△/×	○/×	○/×	○/×	○/×	○/×[1]
3	×/×	△/×	○/×	○/×	○/×	○/×	○/×
3.69 (unadjusted)	×/×	△/×	○/×	○/×	○/×	○/×	○/×
5	×/×	△/×	○/×	○/×	○/×	○/×	○/×
6	△/×	○/×	○/×	○/×	○/○	○/○*	○/○*,[2]

[a] "×, △ and ○" before the slash represent no turbidity, slight turbidity and notable turbidity, respectively, while "× and ○" behind the slash represent no aggregation and visible aggregation-phase separation, respectively (The superscript of asterisk denotes the loss of re-dispersability of the pellet after centrifugation)
[b] Zeta potential (mV): 1. 23.03±1.358; 2. 4.785±0.205 [43]

negative sulfate ion increases as a pH increases. As the mass ratio of chitosan and fucoidan increases at pH 6 of the chitosan solution, the negative charge density of fucoidan molecules in each chitosan-fucoidan nanoparticle becomes comparable to the positive charge density of its chitosan molecules, which brings about most extensive intermolecular electrostatic interactions and leads to the formation of visible intermolecular aggregation during the formation of polyelectrolyte complexes as shown in Table 2. Therefore, the turbidity and the yield of chitosan-fucoidan nanoparticles turn out to be the greatest at pH 6 in the given pH range, as shown in Figs. 2 and 3, respectively. In addition, at pH 6 it resulted in the shift of turbidity/aggregation pattern at the lower pH to the left in Table 2. Thus, at pH 6, such high chitosan-fucoidan mass ratios of 1 : 0.6, 1 : 0.8 and 1 : 1 lead to visible aggregation during the formation of polyelectrolyte complexes unlike the low chitosan-fucoidan mass ratios of 1 : 0.05, 1 : 0.1, 1 : 0.2 and 1 : 0.4. It is attributed to that positive free net charge density of chitosan-fucoidan nanoparticles formed by polyelectrolyte complexation becomes less as the pH of solution gets higher or their mass ratio of solution gets higher up to 1 : 1. It is consistent with the observation of Gan et al. [9] that the charge density of chitosan molecules is dependent on the pH of solution. It is suggested that a stoichiometric ratio between positive amino groups and negative sulfate ions of prepared chitosan-fucoidan nanoparticles is proportionally correlated with the ratio of positive amino groups and negative sulfate ions in a mixed solution prior to polyelectrolyte complexation. This is experimentally substantiated in the ensuing section of this article that a fucoidan-loading efficiency tends to increase as the corresponding chitosan-fucoidan mass ratio increases. It is also supported by the zeta potential measurement of chitosan-fucoidan nanoparticles at different pH environment as shown in Fig. 4. The value of zeta potential measured at pH 6 is lower than that at any lower pH environment and tends to decrease and to approach "zero" or iso-electric point (IEP) as a mass ratio of chitosan-fucoidan increases up to 1:1, which leads to forming a visible aggregation of polyelectrolyte complexes, as shown in Table 2. Nevertheless, according to Fig. 4, chitosan-fucoidan nanoparticles prepared at pH 6 carry a positive charge as long as the mass ratio of chitosan-fucoidan remains less than or equal to 1 : 1 (i.e., 1 : 0.2-1 : 1). However, chitosan-fucoidan nanoparticles prepared at pH 7 as well as pH 7.4 turn out to carry a negative charge in most mass ratio-ranges less than 1 : 1. This confirms that the applied ranges of pH as well as of the mass ratio of chitosan and fucoidan in this

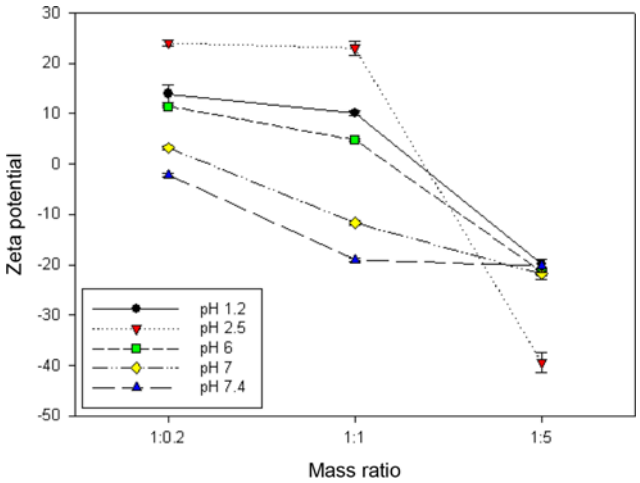

Fig. 4. Zeta potential of chitosan-fucoidan nanoparticles prepared by polyelectrolyte complexation [43].

investigation are quite adequate in order to render the prepared chitosan-fucoidan nanoparticles to keep positive free net charge densities.

Since the charge density of chitosan molecules is dependent on the pH of solution [9], at pH 2 of the chitosan solution, the protonation of the amino groups of chitosan is quite sufficient for neutralizing the sulfate groups of fucoidan. Therefore, at pH 2 of the chitosan solution the concentration of the sulfate groups from fucoidan which is proportional to the chitosan-fucoidan mass ratios (1 : 0.05-1 : 1), is believed to be much less than the concentration of amino groups of chitosan protonated by hydrogen ion, of which the concentration is bigger O(10^4) times than the concentration of hydrogen ion at pH 6 of the chitosan solution. For that reason, the turbidity and the yields of chitosan-fucoidan polyelectrolyte nanoparticles prepared at pH 2 of the chitosan solution are much less sensitive to the chitosan-fucoidan mass ratios, as shown in Figs. 2 and 3, than those at pH 6 of the chitosan solution.

Since the color of fucoidan is yellowish brown, the turbid suspensions obtained had a yellowish appearance. The yellowish pellets after centrifugation could be easily redispersed into a turbid suspension except for the case of pH 6-chitosan solution and the chitosan-fucoidan mass ratio of 1 : 0.8 or 1 : 1, as shown in Table 2.

3. Estimation of Fucoidan-loading Efficiency

According to Fig. 2, the turbidity resulting from the generated

Table 3. Estimated fucoidan-loading efficiency

pH	Mass ratio	Fucoidan loading efficiency
2	1 : 0.6	0.116 (±0.039)
	1 : 0.8	0.195 (±0.001)
	1 : 1	0.474 (±0.060)
6	1 : 0.2	0.148 (±0.045)
	1 : 0.4	0.375 (±0.052)
	1 : 0.6	0.481 (±0.139)
	1 : 0.8	0.432 (±0.001)
	1 : 1	0.958 (±0.001)

chitosan/fucoidan complex tends to increase as either pH or chitosan/fucoidan mass ratio increases. The fucoidan-loading efficiency was measured at pH of 2 and 6 as lower and upper bound, respectively. To study the practical loading of fucoidan, the range of chitosan/fucoidan mass ratio, applied to estimate the fucoidan-loading efficiency, was determined to be above one, satisfying the turbidity of 0.046, as shown in Fig. 2. Accordingly, the fucoidan-loading efficiency was obtained for the chitosan-fucoidan mass ratios of 1 : 0.2, 1 : 0.4, 1 : 0.6, 1 : 0.8 and 1 : 1 at pH 6 as well as 1 : 0.6, 1 : 0.8 and 1 : 1 at pH 2. The fucoidan-loading efficiencies calculated according to Eq. (2) are shown in Table 3. The fucoidan-loading efficiency generally ranges from 0.1 to 0.5. It is remarkable that fucoidan-loading efficiency approaches 0.96 at the experimental condition of pH 6 and the chitosan-fucoidan mass ratio of 1 : 1. The fucoidan-loading efficiency tends to increase as the corresponding chitosan-fucoidan mass ratio increases. Furthermore, the fucoidan-loading efficiency becomes greater as either the chitosan-fucoidan mass ratio or the pH increases, which resembles the behavioral pattern of turbidity, as shown in Fig. 2.

4. Mean Size of Hydrogel Chitosan-fucoidan Complex Nanoparticles

The hydrogel particle size of the chitosan-fucoidan complex is believed to be dependent on pH as well as the mass ratio of chitosan and fucoidan. The dependencies of hydrogel-particle size on their mass ratio and pH are shown in Fig. 5, at each pH of chitosan solution and their mass ratios, respectively. The polydispersity index for their size distribution is shown in Table 4. The hydrogel particle size of chitosan-fucoidan complex turned out to range from 365 nm to 900 nm. The hydrogel nano-particle-size was the biggest at their mass ratio of 1 : 0.05. The nano-hydrogel particle size of chitosan-fucoidan complex tends to decrease as the mass ratio of chitosan and fucoidan increases up to 1 : 1. It is consistent with the experimental fact that free net positive charge density of hydrogel nanoparticles decreases as the mass ratio of chitosan and fucoidan increases, according to

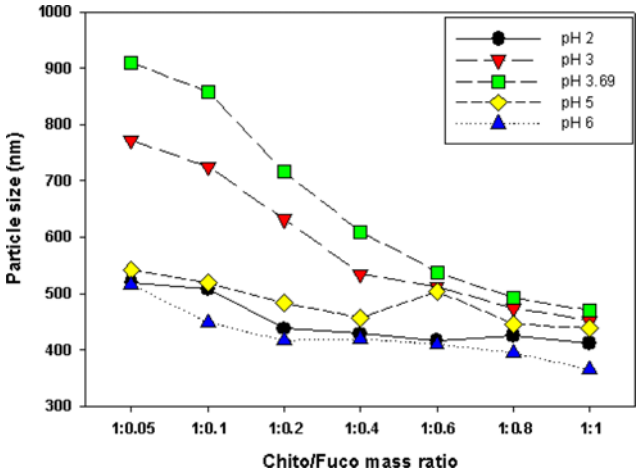

Fig. 5. Effect of chitosan-fucoidan mass ratio at various pH on the size of chitosan-fucoidan complex particle (see Table 4 for polydispersity index).

Fig. 4. Recall that in the previous section a stoichiometric ratio between positive amino groups and negative sulfate ions for the electrostatic reaction of polyelectrolyte complexation is believed to be proportionally correlated with their concentration (or density) ratios in a mixed solution prior to polyelectrolyte complexation. The degree of size-decreasing was the most prominent at pH 3.69 (unadjusted), at which the hydrogel-nanoparticle size ranged from 550 nm to 900 nm and appeared the biggest, at any given mass ratio of chitosan and fucoidan in this study, among those at pH 2, 3, 3.69, 5 and 6. Then pH 3, 5, 2 and 6 were the order of size-decreasing degree as well as nano-particle size at a given mass ratio of chitosan and fucoidan, as shown in Fig. 5. It was more prominent at the less mass ratio of chitosan and fucoidan. In addition, the hydrogel-nanoparticles with the size of ca. 365-450 nm were prepared at any given pH when the mass ratio of chitosan and fucoidan was 1 : 1 as shown in Fig. 5, where the pH conditions of 6 and 2 led to preparing the hydrogel-nanoparticles with the minimum size of 365 nm and the second minimum size of 400 nm, respectively. The hydrogel-nanoparticle size distribution is shown in Fig. 6, where the average size of hydrogel-nanoparticles is a minimum of 365 nm.

5. FTIR Spectrum of Chitosan, Fucoidan and their Complex

Fig. 7(a) shows the FTIR spectrum of chitosan, fucoidan and the chitosan-fucoidan complex (formed with the chitosan solution of pH 2 and the chitosan-fucoidan mass ratio of 1 : 1). Since chitosan and fucoidan are both polysaccharides, their FTIR spectra show the characteristic polysaccharide bands in the region of 900-1,150

Table 4. Polydispersity Index for the size distribution of chitosan-fucoidan complex particle dispersed at various pH and mass ratios

pH	Chitosan-fucoidan mass ratio						
	1 : 0.05	1 : 0.1	1 : 0.2	1 : 0.4	1 : 0.6	1 : 0.8	1 : 1
2	0.385	0.402	0.423	0.364	0.379	0.166	0.219
3	0.352	0.370	0.123	0.385	0.365	0.340	0.354
3.69 (unadjusted)	0.305	0.225	0.189	0.313	0.410	0.321	0.248
5	0.117	0.065	0.261	0.290	0.244	0.215	0.249
6	0.154	0.190	0.264	0.255	0.233	0.267	0.223

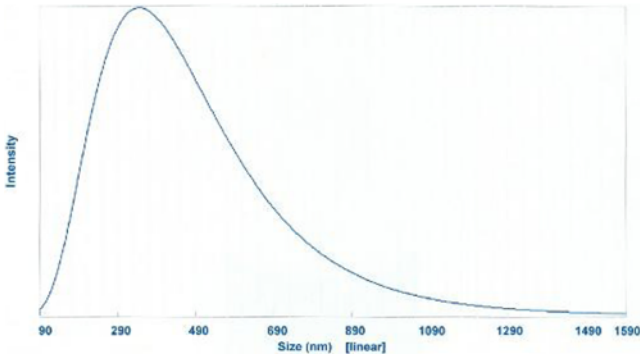

Fig. 6. Size distribution of chitosan-fucoidan complex particle with unimodal size mean of 365.3 nm at the chitosan-fucoidan mass ratio of 1 : 1 and pH 6.

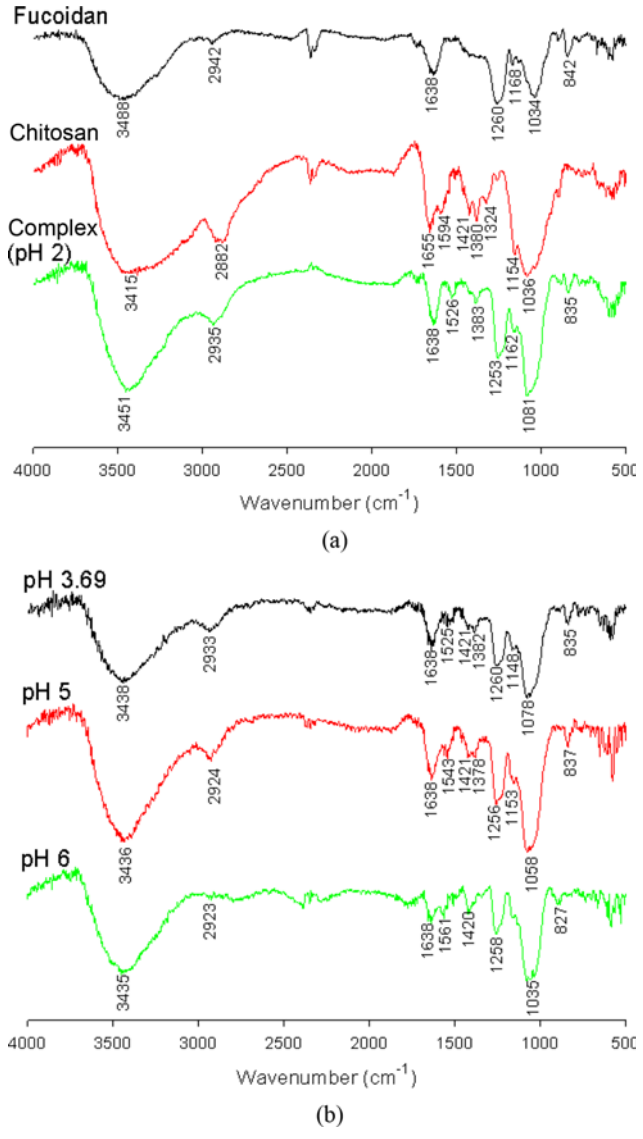

Fig. 7. FT-IR spectrum of fucoidan, chitosan and their complexes: (a) Fucoidan, chitosan and their complex formed with the chitosan solution of pH 2 and the chitosan-fucoidan mass ratio of 1 : 1; (b) Chitosan-fucoidan complexes formed with the chitosan solutions of pH 3.69 (unadjusted), 5 and 6, and the chitosan-fucoidan mass ratio of 1 : 1.

cm^{-1}, which corresponds to the ring stretching, C-O stretching, asymmetric bridge oxygen stretching of the saccharide structure [48-50]. Besides, both have characteristic peaks at 2,880-2,950 cm^{-1} and 3,400-3,500 cm^{-1}, which are attributed to the presence of aliphatic and hydroxyl groups, respectively [51,52]. Despite the above similarities in the structure of chitosan and fucoidan, they both have typical peaks for their characteristic groups. For instance, the characteristic peak at 1,594 cm^{-1} in the spectrum of chitosan is attributed to the amino groups and those at 1,655 cm^{-1}, 1,380 cm^{-1} and 1,324 cm^{-1} are attributed to amide I, amide II, amide III bands, respectively [1,48,53-55]. On the other hand, the spectrum of fucoidan has a special peak at 1,260 cm^{-1}, which represents the S=O stretching of the sulfate group and the additional peak at 842 cm^{-1} attributed to the O-4 sulfates [56]. The peak at around 1,638 cm^{-1} in the spectrum of fucoidan may be due to the presence of 2-O-acetyl groups in the structure [34,51,57]. The spectrum of the chitosan-fucoidan complex (formed with the chitosan solution of pH 2 and the chitosan-fucoidan mass ratio of 1 : 1) shows that the amide I and amide III bands of chitosan (at 1,655 cm^{-1} and 1,324 cm^{-1}, respectively,) are completely absent and have presumably shifted nearby in the spectrum. In addition, the amino group peak of chitosan at 1,594 cm^{-1} has also disappeared. However, a new peak at 1,526 cm^{-1}, shifted from the amino group-peak of 1,594 cm^{-1}, has appeared. The peak at 842 cm^{-1} attributed to the O-4 sulfates of fucoidan has shifted to 835 cm^{-1}. The peaks at 1,383 cm^{-1}, 1,253 cm^{-1} and 1,638 cm^{-1} corresponding to the amide II shifted from 1,380 cm^{-1} of chitosan, the S=O stretching of the sulfate groups shifted from 1,260 cm^{-1} of fucoidan and 2-O-acetyl groups of fucoidan, respectively, are still present in the structure. Due to the polysaccharide nature of both the polymers, the common saccharide peak at 900-1,150 cm^{-1}, hydroxyl peak around 3,400 cm^{-1} and aliphatic peak around 2,900 cm^{-1} are present in all the cases. However, in the case of the chitosan-fucoidan complex formed with the chitosan solution of pH 2, its FT-IR spectrum resembles the spectrum of hyaluronic acid where the hydroxyl peak is observed as severely interfered with by an aliphatic peak unlike chitosan. It can indicate that the hydroxyl peak comes from the carboxylic acid entrapped within the hydrogel of the chitosan-fucoidan complex.

Fig. 7(b) shows the FTIR spectrum of chitosan-fucoidan complexes (formed with the chitosan solutions of pH 3.69 (unadjusted), 5 and 6, and the chitosan-fucoidan mass ratio of 1 : 1). Like the FTIR spectrum of the chitosan-fucoidan complex formed with the pH 2-chitosan solution in Fig. 7(a), the peaks at 1,382 cm^{-1}, 1,260 cm^{-1} and 1,638 cm^{-1} corresponding to amide II of chitosan, and S=O stretching of the sulfate groups and 2-O-acetyl groups of fucoidan, respectively, are still present; the shifted peak of amino group at 1,525 cm^{-1} has still appeared; the peaks of amide I and amide III of chitosan at 1,655 cm^{-1} and 1,324 cm^{-1}, respectively, are still completely absent and have presumably shifted nearby in the spectrum of chitosan-fucoidan complex formed with pH 3.69 (unadjusted)-chitosan solution. The peaks at 3,400-3,500 cm^{-1}, 2,900-2,950 cm^{-1} and 900-1,150 cm^{-1} are still all present in the FTIR spectrum. Unlike the FTIR spectrum with the pH 2-chitosan solution, a new peak at 1,421 cm^{-1} appears in the spectrum, which might have come from the spectrum of chitosan and is attributed to the C-H bond of aliphatic groups [51].

Chitosan-fucoidan complex formed with pH 5-chitosan solution shows the same pattern of absorbance as those with the pH 3.69

(unadjusted)-chitosan solution except that both peaks of the amino group at 1,594 cm^{-1} and amide II at 1,380 cm^{-1} in the spectrum of chitosan solution, are shifted to 1,543 cm^{-1} and 1,378 cm^{-1}, respectively. Moreover the peaks of S=O stretching of the sulfate groups and O-4 sulfates of fucoidan at 1,260 cm^{-1} and 842 cm^{-1} have shifted to 1,256 cm^{-1} and 837 cm^{-1}.

With regard to chitosan-fucoidan complex formed at pH 6, all the amide I, amide II, amide III peaks of chitosan at 1,655 cm^{-1}, 1,380 cm^{-1}, 1,324 cm^{-1}, respectively, are completely absent. Thus, the involvement of amide groups in the electrostatic interaction is evident, which may be through the hydrogen bonding interaction. The peak of the amino group of chitosan at 1,594 cm^{-1} has shifted to 1,561 cm^{-1}, and the peaks of S=O stretching of the sulfate groups and O-4 sulfates of fucoidan at 1,260 cm^{-1} and 842 cm^{-1} have shifted to 1,258 cm^{-1} and 827 cm^{-1}.

It is interesting that as the pH of chitosan solution was increased from 2 to 6, the amino group-peak of chitosan at 1,594 cm^{-1} shifted, as shown in Fig. 7: with pH 2 and 3.69-chitosan solution, to the furthest right of FT-IR spectrum at 1,526 cm^{-1} and 1,525 cm^{-1}, respectively; with pH 5-chitosan solution, to the further right of FT-IR spectrum at 1,543 cm^{-1}; with pH 6-chitosan solution, to the right of FT-IR spectrum at 1,561 cm^{-1}. Moreover, as the pH of chitosan solution was increased from 2 to 6, the O-4 sulfate group-peak of fucoidan at 842 cm^{-1} was shifted as shown in Fig. 7; with pH 2, 3.69 and 5-chitosan solution, to the right of FT-IR spectrum at 835-837 cm^{-1}; with pH 6-chitosan solution, to the further right of FT-IR spectrum at 827 cm^{-1}. Thus the shifts of the amino group-peak of chitosan and the O-4 sulfate group-peak of fucoidan show a correlation with the pH of the chitosan solution. However, there seems to be no correlation between the shift of S=O stretching peak of the sulfate group of fucoidan, and the pH of the chitosan solution.

6. Morphology of Chitosan-fucoidan Complex

The hydrogel-nanoparticles of the chitosan-fucoidan complex were prepared at the mass ratio of chitosan and fucoidan of 1 : 1 and at pH 6 to have the minimum size of 365 nm. It is well known that lyophilization induces inter-nanoparticle aggregation during the freezing step due to significant entanglement of polymer chains as the freezing interface propagates [58]. Instead of lyophilizing the hydrogel-nanoparticles, one drop of their suspension was placed on glass and was dried at room temperature to avoid forming a freeze-drying-induced nanoparticle-matrix. The prepared chitosan-fucoidan complex nanoparticles were observed by a field emission scanning electron microscope (Hitachi, S-4300) as shown in Fig. 8. Their nanoparticle-shape was observed as not uniform consisting of round, rectangular and oval morphologies.

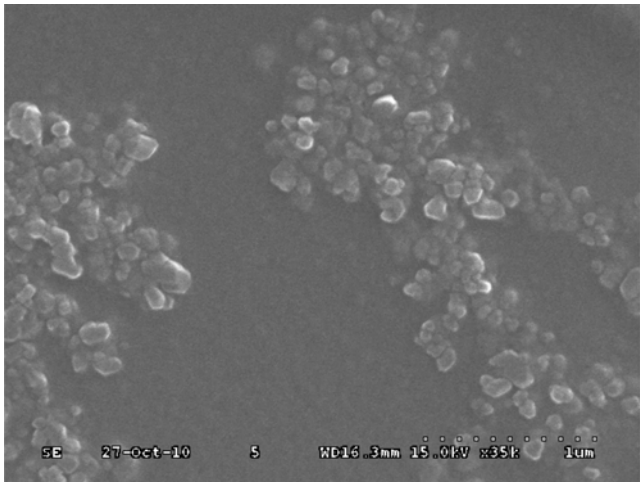

Fig. 8. Chitosan-fucoidan complex nanoparticles, dried in air on glass slide, observed by field emission scanning electron microscope (Hitachi, S-4300): chitosan solution of pH 6 and chitosan-fucoidan ratio of 1 : 1.

7. Proposed Optimum Condition to Prepare Chitosan-fucoidan Nanoparticles

In the previous section of this article it was confirmed that the applied ranges of pH as well as of the mass ratio of chitosan and fucoidan in this investigation are quite adequate in order to render the prepared chitosan-fucoidan nanoparticles to keep positive free net charge densities. Furthermore, the system in this investigation turned out to approach IEP, causing visible aggregation of polyelectrolyte complexes as a mass ratio of chitosan-fucoidan increased to 1 : 1 at pH 6. Therefore, the occurrence of a visible aggregation should be regarded as that the prepared chitosan-fucoidan nanoparticles in this investigation lost their positive free net charge density.

Since smaller positively-charged chitosan nanoparticles are believed to promote intestinal uptake more greatly, the environment of pH 6 may meet the optimum condition to prepare the nanoparticles with a high yield. However, it was observed that at the environment of pH 6, their suspension is so unstable that aggregation may occur at the chitosan-fucoidan mass ratio of 1 : 0.6, 1 : 0.8 and 1 : 1, as shown in Table 2 and Fig. 4. Then pH 2 may be an alternative optimum condition. However, the yield of chitosan-fucoidan nanoparticles was as little as less than ca. 20% as shown in Fig. 3. Thus, both pH conditions of 6 and 2 were discarded. Then, pH 5 was designated as the ad hoc optimum condition to satisfy both the stable suspension and the yield of at most 35% (at the chitosan-fucoidan mass ratio of 1 : 1), as shown in Table 2 and Fig. 3, respectively. In addition, the proposed ad hoc optimum conditions were apparently found to satisfy the condition of the smallest mean-size of chitosan-fucoidan nanoparticles as well, except for the pH environment of 6 and 2, as shown in Fig. 5.

The second order polynomial equation (quadratic) to consider the main effect, quadratic effect and interactive effect of independent variables was fitted to the combined observation (1000 times Y/δ^n) obtained on the basis of a central composite design (CCD) for the optimization of the values of chitosan-fucoidan nanoparticles prepared per unit input mass with the power index (n) values of 1, 3/2, 2 and 3. The physical meaning of increasing the value of n is interpreted as that the mean size of chitosan-fucoidan nanoparticles (δ) is treated with a heavier weight than the yield of chitosan-fucoidan nanoparticles (Y) in terms of combined observation (1000 times Y/δ^n). The adequacy and fitness of the model was tested by analysis of variance (ANOVA) as shown in Table 5 and Table 6. In case that the values of n are equal to 1 or 3/2, significance probability (i.e., *P*-value) of each parameter coefficient exceeds the significance level of 0.03. Then the second order polynomial equations (quadratic) obtained in terms of coded factors are given, in case of n=2 and 3, as Eqs. (6) and (7).

$$\eta_2 = 0.1003 + 0.0835x_1 + 0.0576x_2 + 0.0928x_1^2 + 0.0343x_1x_2 - 0.0082x_2^2 \quad (6)$$

Table 5. Analysis of variance for the response surface quadratic model on the basis of an individual term

Source	η_1 (n=1)		$\eta_{3/2}$ (n=3/2)		η_2 (n=2)		η_3 (n=3)	
	RC	*P*-value	RC	*P*-value	RC	*P*-value	RC	*P*-value
Model	59.5444	<0.04	2.7556	<0.03	0.1285	<0.02	0.0003	<0.01
Intercept	52.9556	0.3781	2.3111	0.2540	0.1003	0.1740	1.87×10^{-4}	0.0832
X_1	33.5833	0.1971	1.7000	0.0977	0.0835	<0.05	2.06×10^{-4}	<0.02
X_2	23.1833	0.9078	1.1667	0.8594	0.0576	0.9060	1.36×10^{-4}	0.9892
X_1X_2	17.1000	0.4804	0.8000	0.4443	0.0343	0.4717	7.00×10^{-5}	0.4716
X_1^2	25.7833	0.1187	1.5917	<0.05	0.0928	<0.03	2.84×10^{-4}	<0.01
X_2^2	−6.0167	0.6478	−0.2583	0.6468	−0.0082	0.7423	-2.50×10^{-6}	0.9616
CV %	15.8666		10.5237		9.5478		8.3565	
R^2	0.9479		0.9643		0.9720		0.9813	

[a] RC, η_n, x_1, x_2, CV and R^2 denote response coefficient, response with the power index of n, pH, mass ratio (MR) of chitosan and fucoidan, coefficient of variation and coefficient of determination, respectively

Table 6. Analysis of variance for the response surface quadratic model by grouping terms

	η_1 (n=1)			$\eta_{3/2}$ (n=3/2)			η_2 (n=2)			η_3 (n=3)		
Regression	R^2	*F* value	*P*-value	R^2	*F* value	*P*-value	R^2	*F* value	*P*-value	R^2	*F* value	*P*-value
Linear	0.7665	22.07	0.0161	0.7329	30.76	0.0100	0.6954	37.32	0.0076	0.6265	50.21	0.0049
Quadratic	0.1702	4.90	0.1135	0.2222	9.33	0.0516	0.2700	14.49	0.0287	0.3506	28.10	0.0114
Interaction	0.0112	0.65	0.4804	0.0092	0.77	0.4443	0.0066	0.71	0.4617	0.0042	0.67	0.4716
Model	0.9479	10.92	0.0385 (<0.04)	0.9643	16.19	0.0222 (<0.03)	0.9720	20.86	0.0155 (<0.02)	0.9813	31.46	0.0085 (<0.01)

[a] η_n and R^2 denote response with the power index of n and coefficient of determination, respectively

$$\eta_3=1.87\times10^{-4}+2.06\times10^{-4}x_1+1.36\times10^{-4}x_2 +2.84\times10^{-4}x_1^2+7.00\times10^{-5}x_1x_2-2.500\times10^{-6}x_2^2 \quad (7)$$

where η_n, x_1 and x_2 are a response (i.e., dependent variable) with the power index of n, pH, a mass ratio (MR) of chitosan and fucoidan.

The coefficient of determination (R^2) was obtained to check the adequacy and fitness of the model. The value of R^2 was calculated to be 0.9720 and 0.9813 for n=2 and 3, respectively, which implies that 97.20% and 98.13% of observation were compatible, respectively. Both small model *P*-values of (<0.02 and <0.01) and high R^2s of 0.9720 and 0.9831 show that the second order polynomial models are significant and sufficient to represent the actual relationship between the response and independent variables for the combined observations with n=2 and 3, respectively. According to Table 5, the significance probabilities (i.e., *P*-values) of a parameter coefficient for the combined observations with n=2 and 3 are less than 0.03 and 0.01, respectively, for the square term of pH (i.e., x_1) and are less than 0.05 and 0.02, respectively, for the linear term of pH (i.e., x_1), which indicates that those terms are statistically significant. According to Table 6, *P*-values of linear terms of the model are 0.0161, 0.0100, 0.0076 and 0.0049 for n=1, 3/2, 2 and 3, respectively, while *P*-values of quadratic terms of the model are 0.1135, 0.0516, 0.0287 and 0.0114 for n=1, 3/2, 2 and 3, respectively. As the value of n decreases R^2 and *F* values of the model decrease and the associated *P*-values increase. It indicates that the model for the combined observations with n=3 becomes more significant than the model with n<3. Thus, the model becomes more significant when the mean size of chitosan-fucoidan nanoparticles (δ) is treated with a heavier weight than the yield of chitosan-fucoidan nanoparticles (Y) in terms of combined observation (1000 times Y/δ^n).

The response surfaces of the model-predicted values (1000 times Y/δ^n) of chitosan-fucoidan nanoparticles prepared per unit input mass are shown in Figs. 9 and 10 with n of 2 and 3, respectively, reflecting the interaction effect between pH and a mass ratio. The condition of pH 6 at the chitosan-fucoidan mass ratio of 1 : 0.6, 1 : 0.8 and 1 : 1 is screened out from optimum pH conditions since the suspension is so unstable that aggregation may occur. As a result, the surface of responses show the maximums values of chitosan-fucoidan nanoparticles prepared per unit input mass at both of pH 5 and the mass ratio of 1 : 1 or at both of pH 6 and the mass ratio between 1 : 0.4, as shown in Figs. 9 and 10 regardless of the value of n. Hence, with exclusion of the condition of pH 6 due to the possible instability of suspension, the proposed ad hoc optimum conditions of pH 5 and the mass ratio of 1 : 1, satisfying both a high yield without aggregation and a small mean size of chitosan-fucoidan nanoparticles, were almost consistent with the optimum conditions derived by RSM for the maximized value of chitosan-fucoidan nanoparticles prepared per unit input mass.

CONCLUSIONS

The effect of the chitosan-fucoidan ratio becomes greater on the yield of the chitosan-fucoidan complex as the pH of chitosan solution is increased. Most of the studied chitosan-fucoidan mass ratios yielded turbid suspension without visible aggregation at all the studied pH condition of chitosan solution except for the mass ratios of

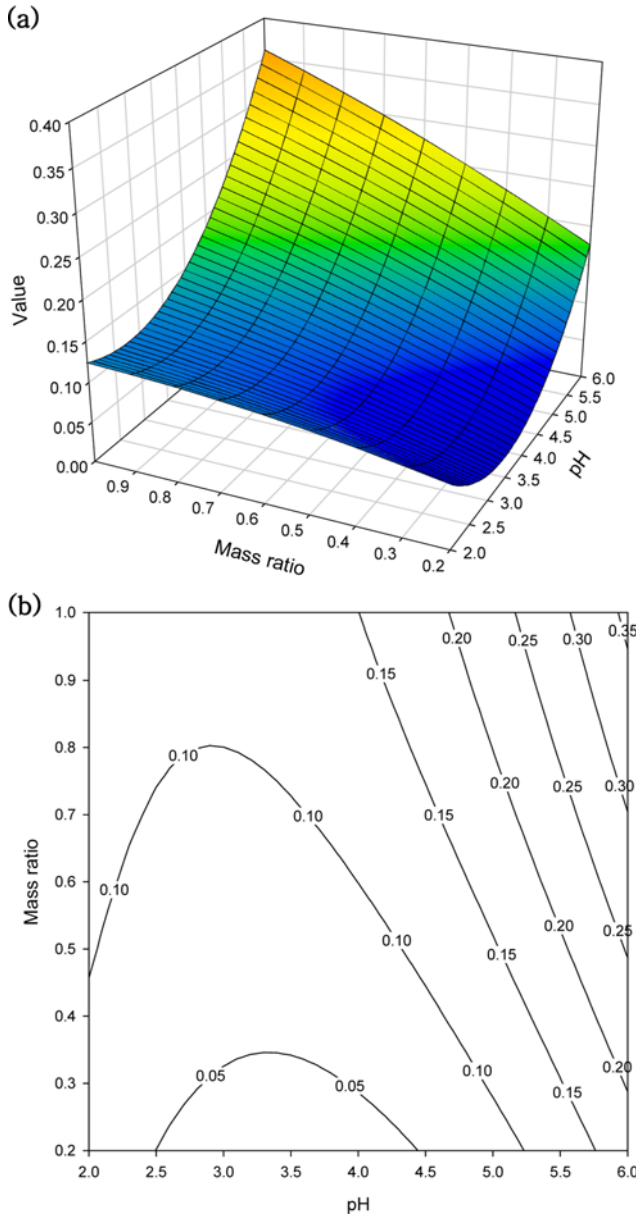

Fig. 9. Response surface plot (a) and contour (b) for the model-predicted values (1000 times Y/δ^2) of chitosan-fucoidan nanoparticles prepared per unit input mass: Y and δ denote yield of chitosan-fucoidan nanoparticles and their mean size, respectively.

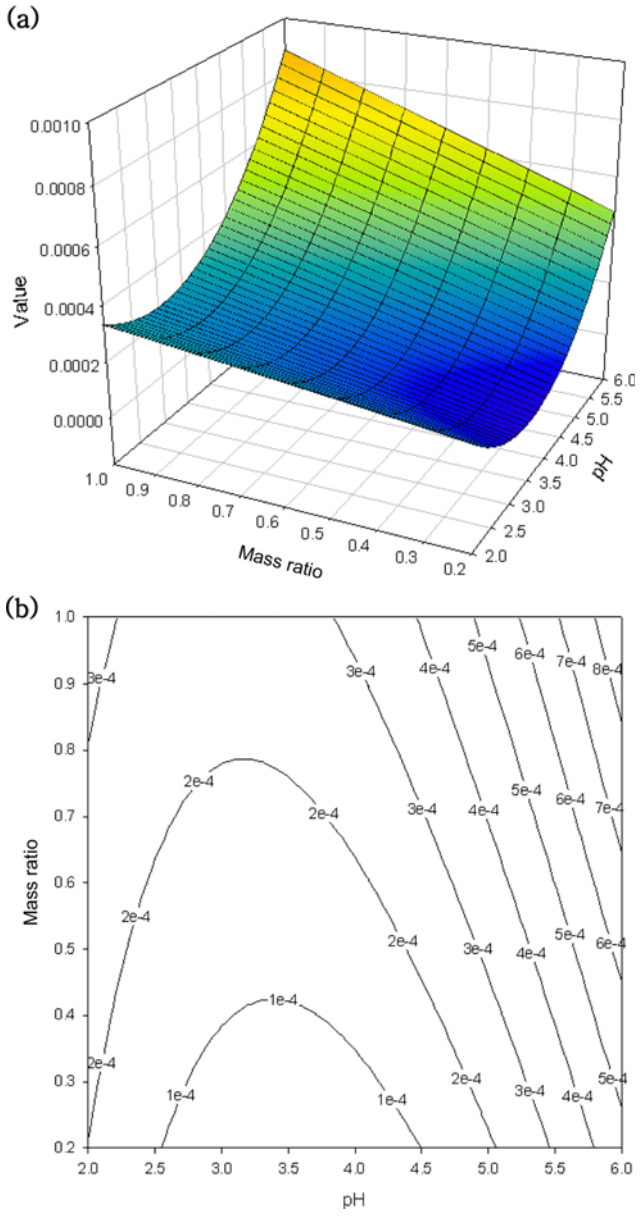

Fig. 10. Response surface plot (a) and contour (b) for the model-predicted values (1000 times Y/δ^3) of chitosan-fucoidan nanoparticles prepared per unit input mass: Y and δ denote yield of chitosan-fucoidan nanoparticles and their mean size, respectively.

1 : 0.6, 1 : 0.8 and 1 : 1 at pH 6, which led to visible aggregates in the suspension. The behavioral pattern of fucoidan-loading efficiency was observed to be similar to that of turbidity, since the sensitivity of fucoidan-loading efficiency to the chitosan-fucoidan mass ratio becomes greater as the chitosan-fucoidan mass ratio and/or the value of pH increases. It illustrates that the turbidity resulting from the formation of the polyelectrolyte complex may be an indirect measure to estimate the loading efficiency of poly-cation or poly-anion into polyelectrolyte complex. At various pH conditions of the chitosan solution, the cationic amino group of chitosan and anionic sulfate groups of fucoidan were found to exist, in FT-IR analysis, whose peaks were shifted according to the pH values of the chitosan solution. Thus, the chitosan-fucoidan complexation occurs due to the electrostatic interaction between the cationic amino group of chitosan and anionic sulfate groups of fucoidan. Nevertheless, the involvement of amide groups in the interaction is also evident, which may be through the hydrogen bonding interaction. The hydrogel particle size of the chitosan-fucoidan complex was observed to range from 365 nm to 900 nm. The hydrogel nano-particle-size was the biggest of ca 900 nm at their mass ratio of 1 : 0.05 and pH 3.69. At the mass ratio of 1 : 1, the pH condition of 6 and 2 led to preparing the hydrogel-nanoparticles with the minimum size of 365 nm and the second minimum size of 400 nm, respectively. The ad hoc optimum conditions of pH 5 and 1 : 1 chitosan-fucoidan mass ratio were

suggested to prepare chitosan-fucoidan nanoparticles satisfying a high yield, small size and good suspension stability. They were almost consistent with the optimum conditions for the maximum value of chitosan-fucoidan nanoparticles prepared per unit input mass, which were analyzed by RSM.

ACKNOWLEDGEMENTS

This research was supported (in part) by the Daegu University Research grant.

REFRENCES

1. J. Du, R. Sun, S. Zhang, L. F. Zhang, C. D. Xiong and Y. X. Peng, *Biopolymers*, **78**, 1 (2005).
2. Y. Chen, V. J. Mohanraj and J. E. Parkin, *Letters in Peptide Science*, **10**, 621 (2003).
3. H. J. Kim, H. C. Lee, J. S. Oh, B. A. Shin, C. S. Oh, R. D. Park, K. S. Yang and C. S. Cho, *J. Biomater. Sci. Polym. Edn.*, **10**, 543 (1999).
4. J. S. Maciel, D. A. Silva, H. C. B. Paula and R. C. M. Paula, *European Polymer Journal*, **41**, 2726 (2005).
5. X. Z. Shu and K. J. Zhu, *Int. J. Pharm.*, **133**, 217 (2002).
6. K. L. B. Chang and J. Lin, *Carbohyd. Polym.*, **43**, 163 (2000).
7. B. Sarmento, S. Martins, A. Ribeiro, F. Veiga, R. Neufeld and D. Ferreira, *Int. J. Pept. Res. Therap*, **12**, 131 (2006).
8. S. A. Agnihotri, N. N. Mallikarjuna and T. M. Aminabhavi, *J. Control Release*, **100**, 5 (2004).
9. Q. Gan, T. Wang, C. Cochrane and P. Mccarron, *Colloids Surf., B: Biointerfaces*, **44**, 65 (2005).
10. X. Yongmei, X. Shufang, D. Yumin and Z. Hua, *Polym. Mater. Sci. Eng.*, **91**, 404 (2004).
11. Y. Aktas, K. Andrieux, M. J. Alonso, P. Calvo, R. N. Gursoy, P. Couvreur and Y. Capan, *Int. J. Pharm.*, **298**, 378 (2005).
12. P. Calvo, C. Remunan-Lopez, J. L. Vila-Jato and M. J. Alonso, *Pharm. Res.*, **14**, 1431 (1997a).
13. P. Calvo, C. Remunan-Lopez, J. L. Vila-JatO and M. J. Alonso, *J. Appl. Polym. Sci.*, **63**, 125 (1997b).
14. T. Lopez-Leon, E. L. S. Carvalho, B. Seijo, L. Ortega-Vinuesa and Bastos-Gonzalez, *J. Colloid Interface Sci.*, **283**, 344 (2005).
15. A. D. E. Salamanca, Y. Diebold, M. Calonge, C. Garcia-Vazquez, S. Callejo, A. Vila and M. J. Alonso, *IOVS*, **47**, 1416 (2006).
16. L. F. Qi, Z. R. Xu, L. Yan, J. Xia and X. Y. Han, *World J. Gastroenterol*, **11**, 5136 (2005).
17. B. Sarmento, D. C. Ferreira, L. Jorgensen and V. De Weert, *Eur. J. Pharm. Biopharm*., **65**, 10 (2007).
18. S. Ichikawa and S. Iwamoto, *Biosci. Biotechnol. Biochem*., **69**(9), 1637 (2005).
19. Z. Liu, Y. Jiao, F. Liu and Z. Zhang, *J. Biomed. Mater. Res. A.*, **83**, 806 (2007).
20. M. Andersson and J. E. Löfroth, *Int. J. Pharm.*, **257**, 305 (2003).
21. H. Q. Mao, K. Roy, V. L. Troung-Le, K. A. Janes, K. Y. Lin, Y. Wang, J. T. August and K. W. Leong, *J. Control Release*, **70**, 399 (2001).
22. Y. Zheng, Y. Wu, W. Yang, C. Wang, S. Fu and X. Shen, *J. Pharm. Sci.*, **95**, 181 (2006).
23. Y. H. Lin, C. K. Chung, C. T. Chen, H. F. Liang, S. C. Chen and H. W. Sung, *Biomacromolecules*., **6**, 1104 (2005).
24. M. E. R. Duarte, M. A. Cardoso, M. D. Noseda and A. S. Cerezo, *Carbohyd. Res.*, **333**, 281 (2001).
25. E. J. Kim, S. Y. Park, J. Y. Lee and J. H. Y. Park, *BMC Gastroenterology*, **10**(96), 1 (2010).
26. T. V. Aleseyenko, S. Y. Zhanayeva, A. A. Venediktova, T. N. Zvyagintseva, T. A. Kuznetsova, N. N. Besednova and T. A. Korolenko, *Bull. Exp. Bio. Med.*, **143**, 730 (2007).
27. D. R. Coombe, C. R. Parish, I. A. Ramshaw and J. M. Snowden, *Int. J. Cancer*, **39**(1), 82 (1987).
28. D. Rou, S. Collec-Jouault, du Sel D. Pinczon, S. Bosch, S. Siavoshian, V. Le Bert, C. Tomasoni, C. Sinquin, P. Durand and C. Roussakis, *Anticancer Res.*, **16**(3A), 1213 (1996).
29. Y. Aisa, Y. Miyakawa, T. Nakazato, H. Shibata, K. Saito, Y. Ikeda and M. Kizaki, *Am. J. Hematol.*, **78**(1), 7 (2005).
30. J. Ye, Y. Li, K. Teruya, Y. Katakura, A. Ichikawa, H. Eto, M. Hosoi, M. Hosoi, S. Nishimoto and S. Shirahata, *Cytotechnology*, **47**, 117 (2005).
31. C. Boisson-Vidal, F. Chaubet, L. Chevolot, C. Sinquin, J. Theveniaux, J. Millet, C. Sternberg, B. Mulloy and A. M. Fischer, *Drug Devel. Res*., **51**, 216 (2000).
32. T. A. McCaffrey, D. J. Falcone, W. Borth, C. F. Brayton and B. B. Weksler, *Biochem. Biophys. Res. Commun*., **184**, 773 (1992).
33. T. Nasu, Y. Fukuda, K. Nagahira, H., Kawashima, C. Noguchi and T. Nakanishi, *Immunol. Lett.*, **59**, 47 (1997).
34. O. Berteau and B. Mulloy, *Glycobiology*, **13**, 29 (2003).
35. P. A. S. Mourao and M. S. Pereira, *Trends Cardiovasc. Med*., **9**, 225 (1999).
36. M. Iqbal, H. Flick-Smith and J. W. McCauley, *J. Gen. Virol.*, **81**, 451 (2000).
37. C. P. Reis, R. J. Neufeld, A. J. Ribeiro and F. Veiga, *Nanomedicine: Nanotechnology, Biology, and Medicine*, **2**, 8 (2006).
38. G. Ranaldi, I. Marigliano, I. Vespigrani, G. Perozzi and Y. Sambuy, *J. Nutr. Biochem.*, **13**, 157 (2002).
39. Z. G. Yue, W. Wei, P. P. Lv, H. Yue, L. Y. Wang, Z. G. Su and G. H. Ma, *Biomacromolecules*, **12**, 2440 (2011).
40. E. J. Lee, S. A. Khan and K. H. Lim, *World J. Eng. Issue Supplement*, 541 (2009).
41. K. Murakami, H. Aoki, S. Nakamura, S.-H. Nakamura, M. Takikawa, M. Hanzawan, S. Kishimito, H. Hattori, Y. Tanaka, T. Kiyosawa, Y. Sato and M. Ishihara, *Biomaterials*, **31**, 83 (2010).
42. Y. C. Huang and T. J. Liu, *Acta Biomater.*, **8**, 1048 (2012).
43. Y. C. Huang and U. I. Lam, *J. Chin. Chem. Soc.*, **58**, 1 (2011).
44. Mitsumata, T., Y. Suemitsu, K. Fujii, T. Fujii, T. Taniguchi and K. Koyama, *Polymer*, **44**, 7103 (2003).
45. G. E. Fredheim and B. E. Christensen, *Biomacromolecules*, **4**, 232 (2003).
46. D. W. Tang, S. H. Yu, Y. C. Ho, F. L. Mi, P. L. Kuo and H. W. Sung, *Biomaterials*, **31**, 9320 (2010).
47. P.-X. Sheng, Y.-P. Ting, J.-P. Chen and L. Hong, *J. Colloid Interface Sci.*, **275**, 131 (2004).
48. Y. J. Yin, K. D. Yao, G. X. Cheng and J. B. Ma, *Polym. Int.*, **48**, 429 (1999).
49. J. E. Santos, E. R. Dockal and E. R. Cavalheiro, *Carbohyd. Polym.*, **60**, 277 (2005).
50. D. Yanming, X. U. Congyi, W. Jianwei, W. Mian, W. U. Yusong and R. Yonghong, *Science in China (Series B)*, **44**, 216 (2001).
51. K. G. Nieman, *Principles of Instrumental Analysis*, **5**, 410 (1998).

52. K. S. H. Yadav, C. S. Satich and H. G. Shivakumar, *Ind. J. Pharm. Sci.*, **69**, 91 (2007).
53. A. C. Chao, S. S. Shyu, Y. C. Lin and F. L. Mi, *Bioresour. Technol.*, **91**, 157 (2004).
54. J. Grant, M. Blicker, M. Piquette-Miller and C. Allen, *J. Pharm. Sci.*, **94**, 1512 (2005).
55. C. Zonggang, M. Xiumei and Q. Fengling, *Mater. Lett.*, **61**, 3490 (2007).
56. L. Chevolot, A. Foucault, F. Chaubet, N. Kervarec, C. Sinquin, A. M. Fisher and C. B. Vidal, *Carbohyd. Res.*, **319**, 154 (1999).
57. J. I. Lee and H. J. Jung, *J. Korean Chem. Soc.*, **49**, 609 (2005).
58. J. Lee, *J. Pharm. Sci.*, **92**, 2057 (2003).